Received September 14, 2018, accepted October 20, 2018, date of publication November 2, 2018, date of current version December 3, 2018.

Digital Object Identifier 10.1109/ACCESS.2018.2879273

A Study on Passive Cooling in Subsea Power Electronics

FAISAL WANI[1], (Student Member, IEEE), UDAI SHIPURKAR[2], (Student Member, IEEE), JIANNING DONG[2], (Member, IEEE), AND HENK POLINDER[1], (Senior Member, IEEE)

[1]Department of Maritime and Transportation Technology, Delft University of Technology, 2628 Delft, The Netherlands
[2]Department of Electrical Sustainable Energy, Delft University of Technology, 2628 Delft, The Netherlands

Corresponding author: Faisal Wani (f.m.wani@tudelft.nl)

This work was supported by the TiPA Project (Tidal turbine Power take-off Accelerator) through the European Union's Horizon 2020 Research and Innovation Programme under Agreement 727793, managed by the Innovation and Networks Executive Agency. This paper reflects only the authors' view; the Agency is not responsible for any use that may be made of the information the paper contains.

ABSTRACT This paper proposes a simplified approach to model the thermal behavior of the insulated-gate bipolar transistors (IGBTs) in a subsea power electronic converter. The models are based on empirical relations for natural convection in water, and IGBT datasheet values. The proposed model can be used in the design of subsea converters and in the reliability analysis of their IGBTs. Experimental results are provided to validate the proposed thermal model. Suggestions are made to minimize the net thermal resistance by introducing a high conductivity thermal material as a mounting plate between the IGBT and the cabinet walls. Impact of the mounting plate dimensions and material properties on the junction temperature of the IGBTs is studied. A case study analysis is made on a 100-kVA converter. Results indicate that the thermal spreading resistances in the mounting plate and the cabinet walls contribute significantly to the overall thermal resistance. Spreading resistances can be mitigated by appropriate design measures. Furthermore, it was observed that the passive cooling in water is not as effective as the forced water cooling. However, the low cost, simple design, and higher reliability of passive cooling systems might make them a favorable choice for subsea systems.

INDEX TERMS Computational fluid dynamics, IGBT, natural convection, submerged power electronics, thermal management of electronics, tidal turbines.

I. INTRODUCTION

A major cause of failure in power electronic converters is the thermally induced stress on semiconductor switches or insulated gate bipolar transistors (IGBTs) [1]–[3]. These failure mechanisms can be mitigated by minimizing the mean junction temperature and the temperature cycling in the IGBTs [1]–[5]. An easy way of doing this is to use forced air or liquid-cooled systems. However, any failure in the cooling system, such as fan/pump malfunction or leakage of the coolant, contribute to the premature failure of the IGBTs [6]. Therefore, periodic maintenance of the cooling system is necessary to minimize downtime and maintenance expenses. As a result, easy access to power electronic systems is favored.

Subsea power electronic converters are required in many applications, such as in oil and gas industry and ocean renewables. For example, a tidal turbine drive train shown in Fig. 1, normally uses a simple 2-level back-to-back voltage source converter (VSC) with IGBTs to control the generator speed/torque, and maintain the active/reactive power balance with the grid. For submerged converters, unforeseen maintenance exercises can be expensive and result in long downtimes. Furthermore, seawater is conductive as well as corrosive; and deployment at significant depths also imposes pressure restrictions. These factors usually increase the failure rates and, consequently, equipment design and ensuring

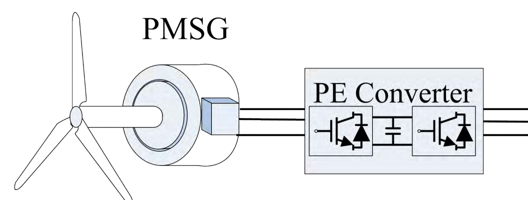

FIGURE 1. Tidal turbine drive train with a direct-drive permanent magnet synchronous generator and a power electronic converter.

2169-3536 © 2018 IEEE. Translations and content mining are permitted for academic research only.
Personal use is also permitted, but republication/redistribution requires IEEE permission.
See http://www.ieee.org/publications_standards/publications/rights/index.html for more information.

reliability is more challenging [7]. Accordingly, most offshore players prefer placing converters onshore, on floating platforms on sea surface, or seabed mounted platforms above the sea surface [8], [9]. Such topologies allow easy access to converters; albeit this comes with increased costs and complexity related to cabling, mooring and platforms, etc.

On the other hand, subsea or seabed mounted converters do not require long and complicated cabling or mooring systems. Besides it potentially makes the control of drives an easier task [10]–[12]. Moreover, seawater provides a heat sink of practically infinite heat capacity. With proper design, passive cooling may provide a more reliable and an inexpensive cooling solution [13]. A simple passive cooling topology for the subsea converter is shown in Fig. 2. Here, the IGBT module is mounted on a plate bolted to the enclosure wall.

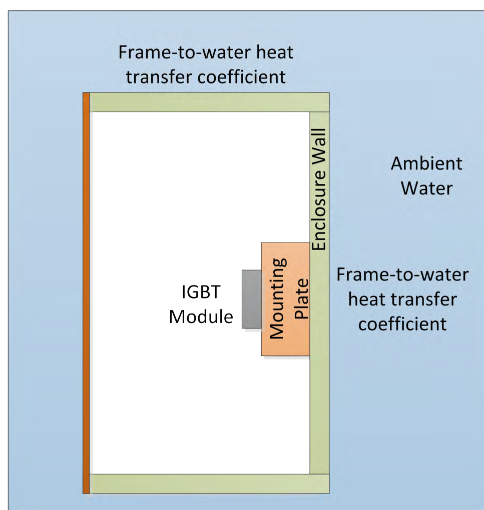

FIGURE 2. A representation of an IGBT module mounted inside a submerged cabinet.

The objective of this paper is to develop a thermal model capable of predicting the dynamic junction temperature of the IGBTs inside a hermetically sealed subsea enclosure. The cooling effect is assumed to be entirely due to the buoyancy-driven flow outside the enclosure or cabinet. Furthermore, the paper identifies the critical parameters that influence the passive cooling characteristics, and suggests measures to improve cooling. The developed model is applied to predict the junction temperature cycling in a 100 kVA tidal turbine power converter. However, for validation purposes, a small scale experimental setup was designed.

Therefore, the primary contribution of this work is the development of a fast analytical thermal model for subsea power electronics and the use of this model in the analysis of passive cooling in subsea power electronics – which is not a widely investigated problem in literature. A secondary contribution is the investigation of the parameters that influence the passive cooling and which results in a good starting point for the design of subsea converters.

The next section revisits the relevant literature on the cooling of power electronics. Section III illustrates the thermal modeling of the IGBTs and the mounting plate in the subsea converter. Section IV explains the calculation of the external heat transfer coefficient using empirical relations. Section V highlights the utility of stationary Computational Fluid Dynamics (CFD) simulations in calculating the heat transfer coefficient. Experimental validation of the thermal models on the scaled down system is demonstrated in Section VI. In section VII, the thermal models are extended to a 100 kVA converter, where a detailed analysis follows on the critical parameters and other aspects of passive cooling. Section VIII summarizes the conclusions drawn from this study, and provides suggestions for future work.

II. LITERATURE REVIEW

Thermal models are necessary for appropriate selection of IGBTs and design of their cooling systems. They are also vital for pre and post-manufacture reliability studies of IGBTs [4], [14], [15]. Forced liquid cooling systems in power electronic converters have been thoroughly investigated in the literature [4], [16]–[20]; and are in common use in many industries. However, passive cooling of the submerged power electronics is not as thoroughly investigated. This is primarily due to fewer subsea applications, and the aforementioned reasons to avoid subsea placement of power electronics.

In a passively cooled subsea system shown in Fig. 2, mainly two modes of heat transfer occur from the IGBT to the cabinet walls: (1) the fluid inside the cabinet undergoes convection (natural or forced) transferring heat to wall; and (2) direct conduction between the heat source and the cabinet walls. In case the IGBT (or heat source) is mounted on a thermally conductive material attached to the wall and the internal medium is air, the bulk of the heat transfer is via the latter mode. The final heat transfer from the cabinet wall to the seawater is by natural convection.

Estimating the flow properties of naturally convecting fluid inside a sealed cabinet is a difficult task. Unlike forced air or liquid cooled systems, the coolant does not continuously enter the system at a constant temperature. As a result numerical techniques such as CFD are used. For instance, Zhang *et al.* [21] analyzed and experimentally verified the temperature distribution inside a high power density sealed flyback adapter using the Flotherm (a commercial CFD package) software. Although computationally expensive, this is by far the most reliable method of guessing the real temperature distribution inside a sealed cabinet, whenever internal convection dominates.

Analytical models have also been developed for thermal modeling of electronics inside a sealed cabinet. However, these models make various simplifying assumptions, which may not hold true in most cases. For example, Teertstra *et al.* [22] modeled the natural convection inside a cabinet with isothermal walls, enclosing a vertical isothermal plate. In this paper, we shall neglect the heat transfer inside the box by natural convection.

In [23], a cold plate based seawater cooling of power electronics in leisure vessels is proposed. The models consider

using filtered seawater as a coolant, whose flow rate in the heat sink channels is determined by the velocity of the vessel. In [24] and [25], seawater is pumped and used as a secondary coolant to cool the freshwater used in central cooling systems of ships. All these systems use seawater in a forced cooling mechanism either directly or indirectly. These models do not analyze cooling systems dependent on natural convection.

Xuan *et al.* [26] consider the cold plate based natural cooling and forced water cooling in maritime generators. They conclude that generators cooled passively should be under rated by almost 40-50% compared to forced cooled generators. This highlights the constraints of relying on natural convection alone.

Kang [27] and Schulz-Harder [28] review the advanced and highly integrated cooling solutions for power electronic devices in their papers. The focus is mainly on forced air and liquid cooling systems. Two-phase cooling and air cooled loop thermosiphon techniques have also been mentioned. However, passive cooling in water is hardly discussed.

Natural convection in vertical channels with asymmetrical heating is addressed in [29]. The paper studies the effect of placing an auxiliary adiabatic plate in the channel on the mass flow rate and heat transfer coefficient. However, the authors restrict themselves to laminar flow regime, and the solution is computed by CFD. Bhowmik and Tou [13] made an experimental analysis on transient natural convection of electronic chips, cooled by water in a vertical up-flow channel driven by buoyancy. In their study, they analyzed the local Nusselt numbers and heat transfer coefficients, and found that the experimental results closely agreed with the available literature on similar geometries. However, in their case they did not consider the impact of spreading resistance in the wall or model the chip temperature.

From above discussion it is clear that passive cooling in submerged electronics is a little investigated problem. Moreover, localized heat sources and thermal spreading resistances in power electronics pose additional complexities in the models. Besides, most of the relevant work seems to rely extensively on CFD simulations. This paper addresses these issues by proposing an approximate—and fast—analytical thermal model.

III. THERMAL MODELS FOR IGBT MODULES AND MOUNTING PLATE

The power converter in Fig. 1 is placed inside a hermetically sealed enclosure. This enclosure could mean a nacelle enclosing a generator as well or a standalone cabinet dedicated to the power converter and other electronic systems. The cabinet must be made of a non-corrosive and thermally conductive material such as Stainless steel 304L.

Referring to Fig. 2, all the heat from the IGBT module is assumed to transfer to the cabinet walls via the mounting plate. For better cooling, a fan may also be installed inside the cabinet; however, we do not consider that here. The bulk of the heat transfer in either case, is expected to be via the mounting plate to the walls.

Three main thermal barriers exist between the IGBT junction and the ambient water. These are: IGBT junction-to-case, case-to-external wall (including mounting plate and enclosure wall), and wall-to-ambient water thermal resistances. A lumped element thermal network for such a system is shown in Fig. 3 . Between these elements, a thin layer of the thermal grease is also usually present; this must be included in the thermal model.

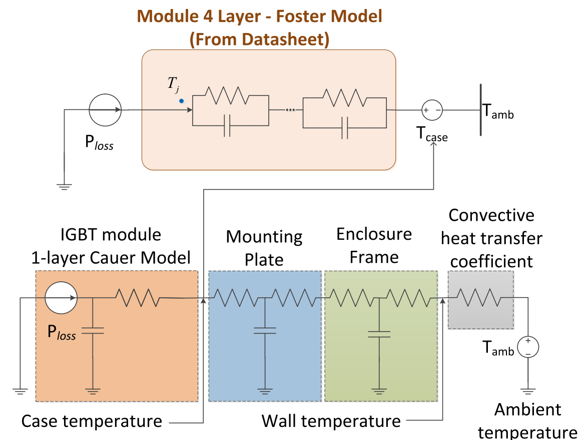

FIGURE 3. Lumped element thermal network model for the system shown in Fig. 2.

The following assumptions are made in this modeling approach:

- Biofouling on the external wall of the enclosure, if any, is assumed to have a negligible impact on the heat transfer coefficient at the wall. Antifouling paints are assumed to work adequately well for the maintenance interval.
- Heat loss via the radiation and the convection inside the box is assumed to be negligible.
- Ambient water around the sealed enclosure is assumed to have zero inherent flow velocity, even though any flow is likely to improve the heat transfer coefficient to the sea. Furthermore, the flow velocity around the box will significantly depend on its mounting position w.r.t the generator/turbine.

The thermal models for the IGBT, the mounting plate, the enclosure walls and the corresponding spreading resistances are addressed below.

A. CAUER AND FOSTER NETWORK MODELS FOR IGBT

In Fig. 3, the IGBT module is represented by a 1-layer Cauer network [30], [31]. Normally, datasheets of IGBT provide the junction-to-case thermal characteristics in the form of multilayer (usually 4) Foster network. However, Foster networks cannot be directly coupled to the mounting plate or heatsink Foster/Cauer networks. On the other hand, using a multilayer Cauer network results in over-filtering of the temperature fluctuations, and thus inaccurate junction temperature estimation [30]. For this reason, we use the two-part combined Foster-Cauer thermal network model as adopted in [4], [30], and [31].

B. MOUNTING PLATE

The IGBT shall normally be placed on a mounting plate made of a thermally conductive material to facilitate the heat transfer to the enclosure wall. The dimensions of the mounting plate and the material has an influence on the thermal resistance, as will be shown later.

The spreading resistance is a crucial component to the total thermal impedance. IGBT acts as a localized heat source on a wider mounting plate. The thermal spreading resistance in the mounting plate also needs to be calculated, in addition to the conventional one-dimensional thermal resistance.

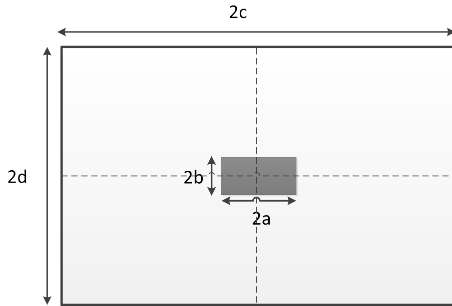

FIGURE 4. Top view of IGBT mounted on a thermally conducting mounting plate. Image is adapted from [32].

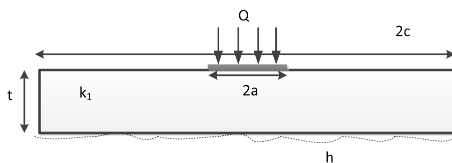

FIGURE 5. Side view of IGBT mounted on a thermally conducting mounting plate. Image is adapted from [32].

Muzychka *et al.* [32] provide a good description of the thermal spreading resistance on rectangular channels. For the system shown in Fig. 4 and Fig. 5, the spreading resistance is given by [32]:

$$\begin{aligned} R_s &= \frac{1}{2a^2cdk_1}\sum_{m=1}^{\infty}\frac{sin^2(a\delta_m)}{\delta_m^3}\cdot\phi(\delta_m) \\ &+ \frac{1}{2b^2cdk_1}\sum_{n=1}^{\infty}\frac{sin^2(b\lambda_n)}{\lambda_n^3}\cdot\phi(\lambda_n) \\ &+ \frac{1}{a^2b^2cdk_1}\sum_{m=1}^{\infty}\sum_{n=1}^{\infty}\frac{sin^2(a\delta_m)sin^2(b\lambda_n)}{\delta_m^2\lambda_n^2\beta_{m,n}}\cdot\phi(\beta_{m,n}) \end{aligned} \tag{1}$$

where, parameters a, b, c and d are defined in Fig. 4; k_1 is the thermal conductivity of the mounting plate. And,

$$\begin{aligned} \delta_m &= \frac{m\pi}{c} \\ \lambda_n &= \frac{n\pi}{d}, \quad \text{and} \\ \beta_{m,n} &= \sqrt{\delta_m^2+\lambda_n^2} \end{aligned} \tag{2}$$

$$\phi(\zeta) = \frac{(e^{2\zeta t}+1)\zeta-(1-e^{2\zeta t})h/k_1}{(e^{2\zeta t}-1)\zeta+(1+e^{2\zeta t})h/k_1} \tag{3}$$

where, h is the heat transfer coefficient at the outer edge of the mounting plate. The lateral faces of the mounting plate are assumed to be adiabatic.

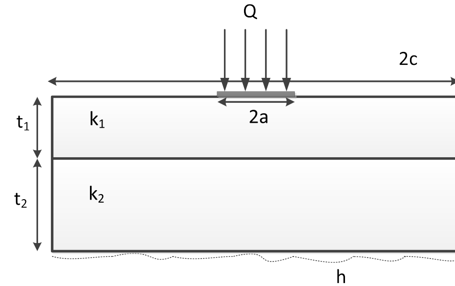

FIGURE 6. IGBT mounted on a thermally conducting base plate made of 2 different layers and/or materials. Image is partially adapted from [32].

For two layers of base plate material, as shown in Fig. 6 the spreading resistance is calculated using the same formulae, however with the following modification [32]:

$$\phi(\zeta) = \frac{(\alpha e^{4\zeta t_1}+e^{2\zeta t_1})+\varrho(e^{2\zeta(2t_1+t_2)}+\alpha e^{2\zeta(t_1+t_2)})}{(\alpha e^{4\zeta t_1}-e^{2\zeta t_1})+\varrho(e^{2\zeta(2t_1+t_2)}-\alpha e^{2\zeta(t_1+t_2)})} \tag{4}$$

where,

$$\begin{aligned} \varrho &= \frac{\zeta+h/k_2}{\zeta-h/k_2} \\ \alpha &= \frac{1-k_2/k_1}{1+k_2/k_1} \end{aligned} \tag{5}$$

In order to account for the thermal resistance of the wall, the parameter, h in (3) and (5) is calculated as follows:

$$\frac{1}{h} = A_{mp}\left(\frac{1}{h_{ext}\ A_{wall}}+\frac{t_{wall}}{k_{wall}\ A_{wall}} + R_{spread,wall}+\frac{t_{tp}}{k_{tp}\ A_{mp}}\right) \tag{6}$$

Here, A_{mp} and A_{wall} denote the areas of the mounting plate and external wall exposed to the seawater. t_{wall} and t_{tp} represent the thickness of the cabinet wall and the thermal paste respectively; whereas, k_{wall} and k_{tp} denote their respective thermal conductivity. $R_{spread,wall}$ denotes the thermal spreading resistance in the wall; and h_{ext} is the external heat transfer coefficient.

The additional thermal spreading resistance in the wall can also be obtained from expressions (1) - (3), with appropriate modifications, as explained in [32]. However, in this case the heat does not spread to the entire wall and careful estimation of the spreading area needs to be made. This point is further explained in the next sections, where the calculation of heat transfer coefficient is explained.

IV. ESTIMATING HEAT TRANSFER COEFFICIENT TO AMBIENT SEAWATER

The heat transfer from the cabinet walls to the ambient water in this case is assumed to be entirely by natural convection. The thermal resistance due to convection is given by,

$$R_{th,conv} = \frac{1}{h_{ext}\cdot A_s} \tag{7}$$

where, h_{ext} is the averaged heat transfer coefficient for the surface area of A_s.

An easy way to estimate the heat transfer coefficient from enclosure wall to the surrounding seawater is by using the empirical relations found in literature [33]–[35]. For modeling the heat transfer due to natural convection, a set of important dimensionless numbers determining the fluid flow regime need to be calculated. These include Grashof number (Gr), Prandtl number (Pr), Rayleigh number (Ra_L), and finally, the Nusselt number (Nu).

For a vertical wall at a temperature T_s, in an ambient fluid of temperature T_∞ at a remote distance from the wall, we have [33]:

$$Gr = \frac{g\beta(T_s - T_\infty)L^3}{\nu^2}$$
$$Pr = \frac{\mu C_p}{k}$$
$$Ra_L = Gr \cdot Pr \tag{8}$$
$$Nu_{T_s} = \left\{0.825 + \frac{0.387Ra_L^{1/6}}{[1 + (0.492/Pr)^{9/16}]^{8/27}}\right\}^2 \tag{9}$$
$$h_m = \frac{Nu \cdot k}{L} \tag{10}$$

where,
g is the acceleration due to gravity (m/s^2) ,
L is the vertical length of the wall (m),
ν is the kinematic viscosity of water (m^2/s),
μ is the dynamic viscosity of water (N·s/m^2),
C_p is the specific heat capacity of water (J/kg·K), and
k is the thermal conductivity of water (W/m·K).

In our case, T_s maybe treated as the mid-point temperature of the wall, and h_m as the mid-point heat transfer coefficient.

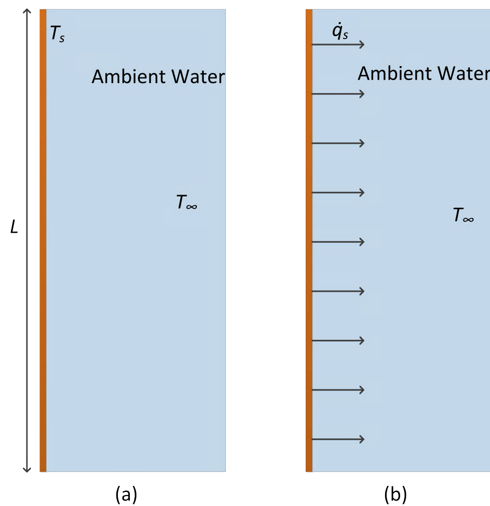

FIGURE 7. A vertical plate exposed to a fluid (a) plate is isothermal; (b) constant heat flux from plate.

The caveat with using the above equation is that the wall temperature T_s must be known *a priori*. However, we can only know the loss from the IGBT, and not the enclosure wall temperature beforehand; see Fig. 7. To circumvent this problem the following approach is adopted here, as suggested in [33] :

1) Assume a certain T_s, and calculate Nu_{T_s} using (8) and (9).
2) For a known value of $\dot{q}_s$, calculate the Nu_{q_s} using the relation,
$$Nu_{q_s} = \frac{\dot{q}_s L}{k[T_s - T_\infty]} \tag{11}$$
3) Iterate T_s value over the previous two steps until $Nu_{T_s} = Nu_{q_s}$.
4) Use (10) to calculate h_m from the converged value of Nu.

The averaged heat transfer coefficient at the vertical edges of the mounting plate can be assumed to be zero, if the heat flux at those edges is taken to be zero. Then the following relation can be assumed:

$$h_{ext} = \frac{h_m}{2}\left(\frac{b_{mp} + b_{hs}}{b_{mp}}\right) \tag{12}$$

where, b_{mp} and b_{hs} denote the horizontal widths of the mounting plate and the heat source respectively. This value of h is used in (6) and (7).

However, there is another problem with the above formulation: the equivalent wall length, L is unknown. Since the heat source is concentrated on the inside of the wall, using the full enclosure wall height as L in (8) and (10) does not seem to be a reasonable approximation. Furthermore, heat from the mounting plate will also not spread equally in vertical direction due to upward flow near the wall. Therefore, determining L becomes critical to the thermal model. Preemptive calculation of L can be done by using CFD, as shown in the next section.

V. OBTAINING EQUIVALENT WALL LENGTH FROM CFD

Strictly speaking, heat transfer from IGBT to the seawater is a 3D conjugate heat transfer problem. CFD simulations can be used to estimate the junction temperature in IGBT modules inside a submerged converter cabinet. However, such models can be extremely time and resource consuming, and are hence, avoided as much as possible.

In this paper, CFD simulations are merely used to estimate the equivalent wall length for heat transfer calculations. Using this information, analytical models based on empirical relations can be used for thermal modeling purposes.

The assumptions and the governing equations for the CFD model of this system are given below.

A. ASSUMPTIONS

– Boussinesq Approximation: In the governing Navier-Stokes equations, density is assumed to be constant except in the buoyancy term. Continuity equation is thus used in its incompressible form. The Boussinesq approximation can be applied under the following condition [36]:
$$\beta(T - T_0) \ll 1 \tag{13}$$

where, β is the thermal expansion coefficient (1/K) , T is the fluid temperature (K), and T_0 is the reference or the operating temperature (K).
A detailed and mathematically rigorous inspection of whether or not the Boussinesq approximation is valid under certain conditions is given in [36] and [37].

- No heat loss to the sea by radiation has been assumed.
- The vertical variation of the heat transfer coefficient derived from 2D CFD modeling is assumed to have similar variation throughout the width of the mounting plate in the horizontal direction. This assumption was made to avoid 3D simulations.

B. GOVERNING EQUATIONS AND BOUNDARY CONDITIONS

The governing differential equations are presented below after applying the Boussinesq approximation.

$$\nabla \cdot U = 0 \tag{14}$$

$$(U \cdot \nabla)U = \nu\nabla^2 U - \frac{1}{\rho}\nabla P - g\alpha\Delta T \tag{15}$$

$$U \cdot \nabla T = \kappa\nabla^2 T \tag{16}$$

where, U is the velocity vector, ν is the kinematic viscosity of water, ρ is the density, P is the pressure, α is the thermal expansion coefficient, T is the temperature, and κ is the thermal diffusivity. Other constants and the material parameters used in the CFD modeling are listed in Table 1.

TABLE 1. Constants and material parameters.

Parameter	Value
Thermal conductivity of Al	170 W/m·K
Thermal conductivity of Cu	400 W/m·K
Thermal conductivity of Stainless steel 304L	15 W/m·K
Thermal conductivity of water	0.6 W/m·K
Thermal conductivity of thermal paste	0.67 W/m·K
Density of water	998 kg/m^3
Density of Al	2700 kg/m^3
Density of Cu	8960 kg/m^3
Density of Stainless steel 304L	7850 kg/m^3
Specific heat capacity of Al	870 J/kg·K
Specific heat capacity of Cu	385 J/kg·K
Specific heat capacity 304L	475 J/kg·K

In addition to the above conservation equations, a turbulence model is required to obtain a solution to the heat transfer problem. In this paper, we use the $k-\epsilon$ model, common in such type of problems [38]. The boundary conditions used at far distance from the box in the sea are the pressure inlet and outlet conditions, at ambient temperatures. ANSYS Fluent was used for CFD simulations, with default parameters for $k-\epsilon$ model.

C. CFD RESULTS

From Fig. 8, it is clear that the heat loss happens mainly only along a part of the vertical wall, and not along the entire wall.

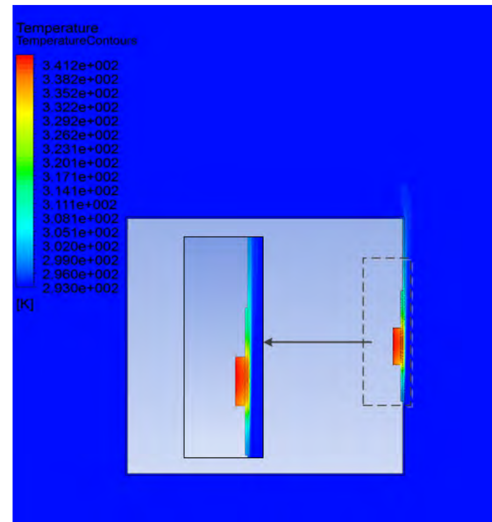

FIGURE 8. Temperature distribution inside the power electronic cabinet.

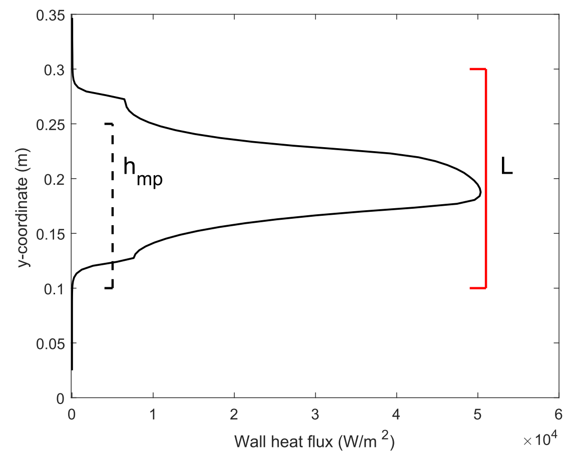

FIGURE 9. Wall heat flux from vertical wall of the box. Equivalent wall length can be obtained from this figure. h_{mp} denotes the vertical length of the mounting plate.

The wall length across which the bulk heat transfer can be obtained as shown in Fig. 9. This wall length is used in (8) - (11).

However, 2D CFD calculations will only give the spreading area in vertical direction. In horizontal direction, the spread can be assumed to be limited to the base plate area owing to the vertical nature of buoyancy-driven flows. The spread of the heat flux may also be assumed to be similar in the horizontal direction as in the vertical direction.

VI. EXPERIMENTAL VALIDATION

Validating the thermal models for the IGBTs rated near the 100 kW level was infeasible in the available laboratory setup. Therefore, a scaled down experimental setup was installed to validate the aforementioned thermal model. In the experiments, normal tap water was used instead of the seawater. Although the models were validated only at low power levels, it is expected that they will be applicable even at higher power levels and larger system dimensions. However, the power

density in the experimental setup was chosen to be around the same value as for the 100 kVA converter.

There is a general consensus on thermal modeling of IGBTs, as mentioned in Section III. The main challenge for submerged power electronics is to estimate the case temperature. For this reason, case or mounting plate temperature is the main focus of the experimental validation.

A. EXPERIMENTAL SETUP

For constant loss in the IGBT, the IGBT can be replaced by any appropriate heat source. A 4.7 Ω resistor was used for this purpose. This was done to generate significant loss on the mounting plate. Commercial IGBTs do not generate such level of loss at low currents and voltages. On the other hand, a simple resistor can easily generate losses upto 60 W from currents less than 4 A, which requires a smaller power supply. The resistor was mounted on an aluminum plate which was then bolted on the enclosure wall. The contact resistance was minimized by applying a thermal grease/paste. The dimensions of the materials used in the experimental setup are listed in Table 2.

TABLE 2. Physical dimensions of the experimental setup.

Parameter	Value
Enclosure wall thickness	0.002 m
Enclosure height	0.350 m
Enclosure width	0.350 m
Enclosure length	0.350 m
Al/Cu Base plate dimensions	0.105 m x 0.150 m
Al Base plate thickness	0.0025 m
Cu Base plate thickness	0.010 m

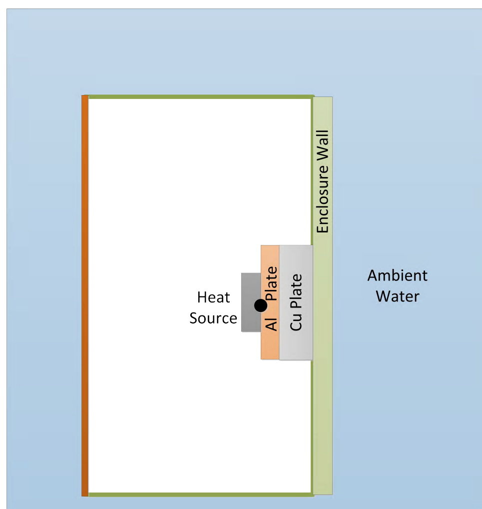

FIGURE 10. Two layers of base plate for mounting of IGBTs. Solid circle represents the thermocouple (temperature sensor) location.

To see the effect of the spreading resistance, an additional copper plate was inserted between the Al plate and the enclosure wall, and the temperature measurements were repeated. The sensor is placed just above the Al plate by making a small groove, as shown in Fig. 10.

B. RESULTS

The following results correspond to an ambient temperature of 24 °C. In the first case, the mounting plate is made only of Al, whereas in the second case, a combination of Al and Cu plate is used.

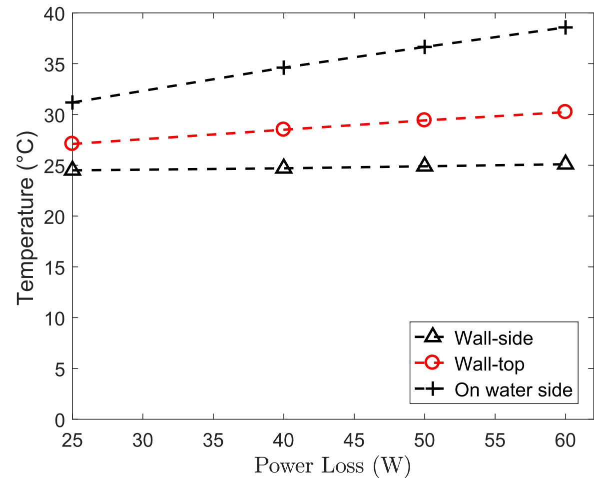

FIGURE 11. Temperatures at different points on the wall. 'Wall-side' and 'Wall-top' denote the temperatures at positions shown in Fig. 12. 'On water side' denotes the temperature on the water side of the wall directly below the heat source.

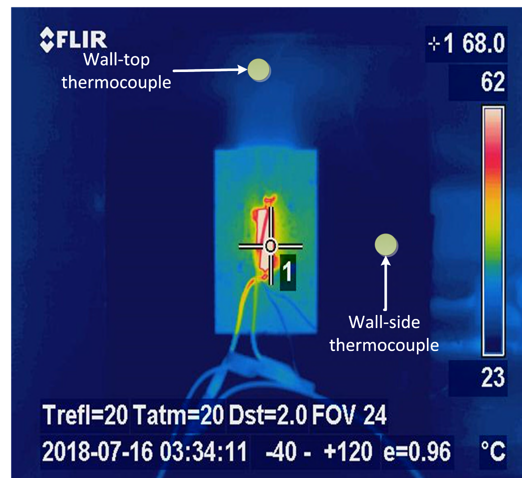

FIGURE 12. Thermal image showing heat spread in aluminum plate and the stainless steel wall. Temperature sensor placement on the walls is also shown by green circles.

1) AL MOUNTING PLATE

Figure 11 shows the temperature measured at different points on the wall of the box for different values of losses in the resistor. The thermal heat spread is shown in Fig. 12. This image also validates the choice of L in (10), and shown in Fig. 9. As seen in Fig. 11, the temperature on the wall sides barely increases indicating that the bulk heat remains concentrated within the width of the mounting plate, mostly flowing vertically upwards in the direction of the buoyancy-driven water flow. The mid-point wall temperature on the water side also increases as expected with the temperature, indicating isothermal boundary condition on the wall is not a suitable approximation to make under these circumstances.

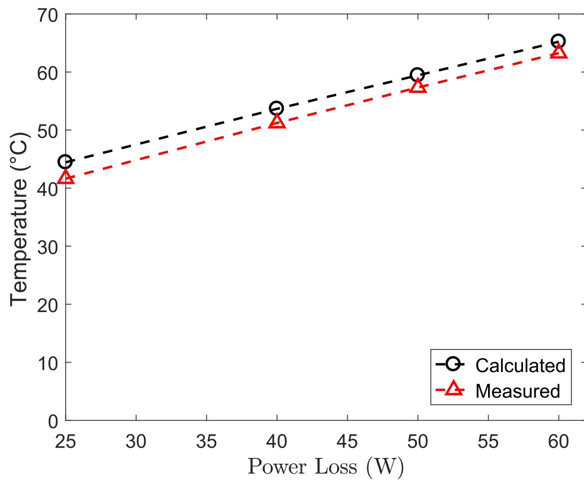

FIGURE 13. Comparison of temperatures between analytical models and measurements below the heat source on the aluminum mounting plate.

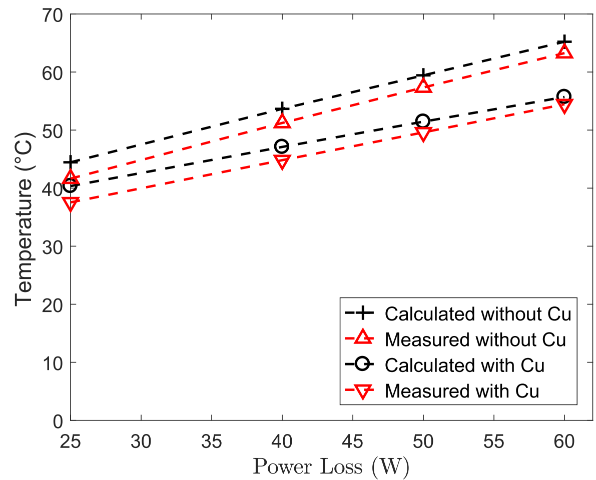

FIGURE 14. Comparison of temperatures between analytical models and measurements below the heat source on the aluminum mounting plate with and without Cu layer.

Figure 13 shows the comparison between the temperature calculated from the model and measured from the setup, at the mid-point just below the heat source.

The errors in the calculated value and the measured value ranged between 5-15%, as calculated from the ambient temperature. These errors can arise from:

- tolerance of sensors;
- placement of sensors (not exactly on top of the Al plate, rather in a trough created on its surface);
- sensor placing also alters the thermal path and hence, affects the thermal resistances; and
- finally, the assumptions made in the modeling, such as neglecting radiation, and less than perfect nature of empirical relations.

2) MOUNTING PLATE MADE OF AL AND CU

The thermal model predicted that the inclusion of the copper layer—in between the cabinet wall and the aluminum plate—should result in the drop of the temperature at Al plate. This was validated by the experimental results, as shown in Fig. 14. The system is similar to that shown in Fig. 10.

The effect of copper layer thickness on the resistor temperature is shown in Fig. 15, as calculated from the model. The marginal utility of increasing the copper layer thickness decreases with increase in thickness. After a certain optimum thickness (in this case around 25 mm), the drop in the spreading resistance by increasing the thickness is overcome by the increase in resistance due to length (also called 1D resistance).

VII. CASE STUDY: ANALYSIS OF A 100 KVA TIDAL TURBINE CONVERTER

In this section, we extend the thermal model to the passively cooled IGBT for a 100 kVA power electronic converter. The converter is assumed to be a 2L back-to-back VSC, with an efficiency of about 97%. The objective is to analyze the characteristics of passive cooling at a larger scale. And consequently, study the contributions of different thermal resistances to the total thermal resistance seen by the IGBT.

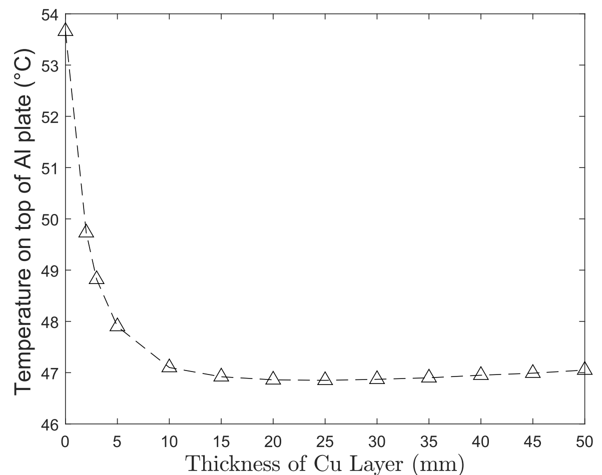

FIGURE 15. Variation of mounting plate temperature with thickness of Cu layer on Al+Cu mounting plate. The loss in the heat source was 40 W.

A. ASSUMPTIONS

The analysis in this section is based on the following assumptions:

- The individual IGBT modules are mounted on separate but closely placed mounting plates in a horizontal array. Since the heat spreads vertically, each IGBT module can be analyzed individually.
- The loss inside a single IGBT has been modeled as a trapezoidal pulsed waveform. For a 100 kVA turbine, the mean power loss in a phase leg of the converter was roughly assumed to be 600 W.
- The aspect ratio of the mounting plate is kept same as that of the IGBT. This is by no means necessary or requirement of the model; it is merely adopted to simplify the calculations, and provide an easily imaginable picture.
- The outer walls of the enclosure are flat, and no biofouling/corrosion layer is considered.
- Ambient temperature of the seawater is 20 °C.

TABLE 3. 100 kVA converter parameters.

Parameter	Value
IGBT dimensions	0.057m x 0.110 m
IGBT R_{th}	[3.8 31.2 0.1 2.0] K/kW
IGBT τ_{th}	[0.0007 0.0247 0.050 3.485] s
Enclosure wall thickness	0.005 m
Enclosure height	1.5 m
Enclosure width	0.5 m
Enclosure length	1.5 m
Cu mounting plate dimensions	0.171 m x 0.330 m
Cu plate thickness	0.010 m
Thermal paste thickness	0.0001 m

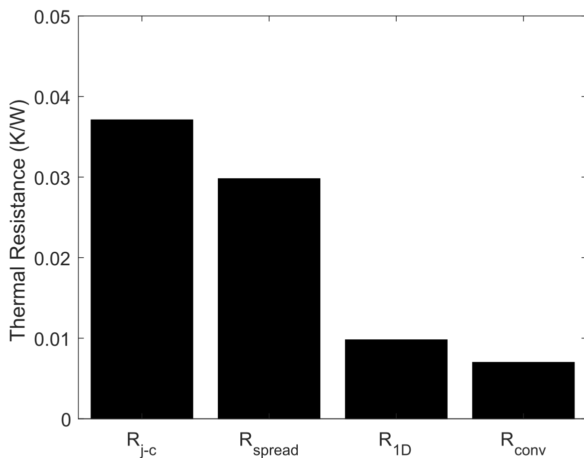

FIGURE 16. Thermal Resistance contributions for mean power loss of 300 W in each IGBT on Generator side of the converter. Mounting plate is made of Cu and is 30 mm thick.

The IGBT (Infineon's FF600R12ME4_B11) used for the analysis is rated at 1200 V and 600 A. The 4-layer Foster network thermal impedance parameters for the IGBT are listed in Table 3, along with the mounting plate and enclosure dimensions.

As mentioned already, we have assumed a constant power loss in the IGBT for our analysis. Under normal circumstances we only know the voltage across and the current in the IGBT. In that case, the IGBT temperature must be used in a feedback loop to calculate the losses.

B. RESULTS

Figure 16 shows the contribution of each thermal resistance component to the overall thermal resistance from the IGBT junction to the ambient seawater. Clearly, the contribution of the spreading resistance to the case-to-ambient thermal resistances is significant.

Suppose that the IGBT is mounted on the copper mounting plate, which is bolted to the cabinet wall. Then for the mounting plate area given in Table 3, the effect of the mounting plate thickness on the IGBT junction temperature is shown in Fig. 17.

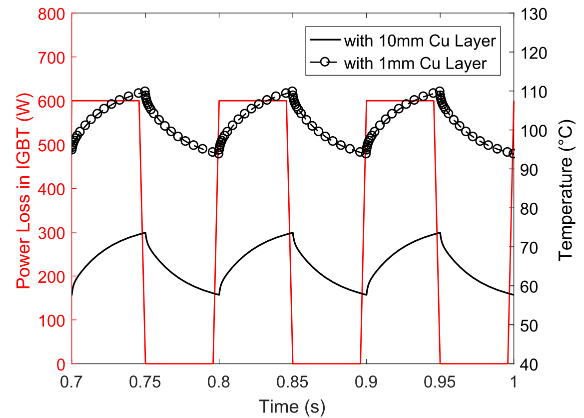

FIGURE 17. IGBT loss and junction temperature (for 100 kVA converter) when mounted on the Cu plate.

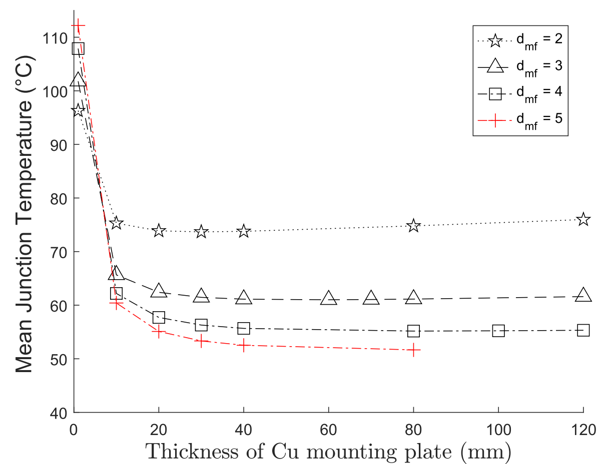

FIGURE 18. Variation of the IGBT mean junction temperature with respect to mounting plate dimensions.

Figure 18 shows the influence of the area of the mounting plate area and thickness on the mean junction temperature of the IGBT. The factor, d_{mf} in Fig. 18, denotes the length multiplying factor of the mounting plate w.r.t the IGBT dimensions. For example, if the IGBT module plate area is 0.057 m x 0.110 m, then d_{mf} of 3 implies the mounting plate dimensions are 0.171 m x 0.330 m (i.e. times 3). The plot shows the same trend as in Fig. 15, although the optimum thickness varies slightly for different values of d_{mf}.

Interestingly, for very small thickness of the mounting plate, increasing the area has opposite effect than at larger thicknesses. A major contributing reason is that the heat transfer coefficient is higher for lower values of d_{mf} ($h_{d_{mf}=2} > h_{d_{mf}=3} > h_{d_{mf}=4} \ldots$). For very small thicknesses, this results in an overall decrease of the spreading resistance, and hence lower mean temperatures.

In Fig. 19, mean junction temperatures are compared for two different mounting plate materials, namely, copper and aluminum. Clearly, the material with higher thermal conductivity has lower spreading resistance, and hence, lower temperature.

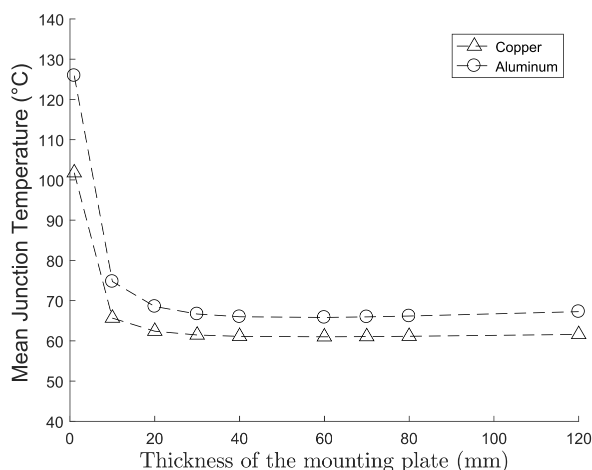

FIGURE 19. Comparison of the IGBT mean junction temperatures based on the mounting plate material; $d_{mf} = 3$.

C. CONCLUSION

From the above discussion, we can conclude the following for the design of the 100 kVA converter:

- Mounting plates made of materials with higher thermal conductivity contribute to the lowering of the junction temperature. However, other factors such as coefficient of thermal expansion must also be taken into account while selecting the mounting plate material.
- The marginal utility decreases with increase in the mounting plate thickness.
- Marginal utility of increasing the d_{mf} also decreases with increase in the value of d_{mf}.
- The optimum mounting plate thickness increases with the increase in d_{mf}.
- Maximum value of d_{mf} in a practical converter will depend on the available space and placement of other devices in the cabinet.
- For the space available in the converter considered here, mounting plate thickness of about 30 mm, and d_{mf} of 3 seems a reasonable choice.

Furthermore, commercial forced water cooling systems usually have a heat sink-to-ambient thermal resistance in the range of 0.005-0.020 W/m·K, whereas forced air cooling systems have this value around 0.1 W/m·K. This implies that cooling efficiency of passively cooled systems in water (in this case, roughly 0.05W/m·K) can be designed to fall between two forced cooling mechanisms. The benefit of passive cooling systems lie in its low cost, simplicity and reliability.

This study considered a flat outer surface of the enclosure. Normally, finned surfaces are known to improve cooling. In the submerged case, especially in the sea, using a finned surface could result in clogging/fouling, and hence overcome the benefits of the increase in surface area. More importantly, thermal resistance due to convection at the surface is only a small component of the total thermal resistance, as shown in Fig. 16. However, finned surfaces devoid of clogging could aid cooling due to the chimney effect [39]. Whether that improvement is significant or not requires a detailed study. For very deep subsea applications, a pressure compensating fluid inside the power electronic cabinet may also be present. Its impact on the cooling of the electronics would be another interesting study to undertake.

VIII. CONCLUSIONS

This paper proposed a thermal model to estimate the junction temperature in an IGBT module cooled by natural convection in water. The model can be used to design the heat sink for the submerged power converters, and in their reliability analysis. The model was experimentally validated on a small scale set up. Assuming that the scale effects do not significantly alter the model, the model was extended to a 100 kVA converter.

Results indicated that the case-to-ambient thermal resistance—especially the spreading resistances in mounting plate and cabinet wall—significantly contributes to the total thermal resistance. However, this will depend on the size of the system, power rating and the IGBT thermal parameters. Mounting plates made of materials with high thermal conductivity (e.g. Cu) can lower the junction temperatures significantly. Also, it was observed that the passive cooling in water is less efficient than the commercially available forced water-cooling systems. Albeit, passive systems are likely to be low cost, simple and more reliable.

The appropriate choice of the cooling system in submerged converters is more complicated. Besides cost and reliability, the designer should also consider the lifetime models of the IGBTs, and the mission profile to which the IGBT is subjected to, etc. A natural extension of this work is to develop models for multiple heat sources inside a sealed cabinet, which includes other heat sources than IGBTs. These studies are currently underway and shall be addressed in a subsequent article.

REFERENCES

[1] S. Yang, A. Bryant, P. Mawby, D. Xiang, L. Ran, and P. Tavner, "An industry-based survey of reliability in power electronic converters," *IEEE Trans. Ind. Appl.*, vol. 47, no. 3, pp. 1441–1451, May/Jun. 2011.
[2] C. Qian *et al.*, "Thermal management on IGBT power electronic devices and modules," *IEEE Access*, vol. 6, pp. 12868–12884, 2018.
[3] M. Andresen, M. Liserre, and G. Buticchi, "Review of active thermal and lifetime control techniques for power electronic modules," in *Proc. 16th Eur. Conf. Power Electron. Appl. (EPE-ECCE Europe)*, Aug. 2014, pp. 1–10.
[4] U. Shipurkar, E. Lyrakis, K. Ma, H. Polinder, and J. A. Ferreira, "Lifetime comparison of power semiconductors in three-level converters for 10-MW wind turbine systems," *IEEE J. Emerg. Sel. Topics Power Electron.*, vol. 6, no. 3, pp. 1366–1377, Sep. 2018.
[5] H. Wang, K. Ma, and F. Blaabjerg, "Design for reliability of power electronic systems," in *Proc. 38th Annu. Conf. IEEE Ind. Electron. Soc. (IECON)*, Oct. 2012, pp. 33–44.
[6] J. Carroll, A. McDonald, and D. McMillan, "Reliability comparison of wind turbines with DFIG and PMG drive trains," *IEEE Trans. Energy Convers.*, vol. 30, no. 2, pp. 663–670, Jun. 2015.
[7] T. Hazel, H. Baerd, J. Legeay, and J. Bremnes, "Taking power distribution under the sea: Design, manufacture, and assembly of a subsea electrical distribution system," *IEEE Ind. Appl. Mag.*, vol. 19, no. 5, pp. 58–67, Sep. 2013.

[8] F. Wani and H. Polinder, "A review of tidal current turbine technology: Present and future," in *Proc. 12th Eur. Wave Tidal Energy Conf. (EWTEC)*, Cork, Ireland, 2017, pp. 1133-1–1133-10.

[9] K. Rajashekara and H. Krishnamoorthy, "Power electronics for subsea systems: Challenges and opportunities," in *Proc. IEEE 12th Int. Conf. Power Electron. Drive Syst. (PEDS)*, Dec. 2017, pp. 986–991.

[10] M. C. Sousounis, J. H. K. Shek, and M. A. Mueller, "Modelling and control of tidal energy conversion systems with long distance converters," in *Proc. 7th IET Int. Conf. Power Electron., Mach. Drives (PEMD)*, Apr. 2014, pp. 1–6.

[11] X. Liang, S. O. Faried, and O. Ilochonwu, "Subsea cable applications in electrical submersible pump systems," *IEEE Trans. Ind. Appl.*, vol. 46, no. 2, pp. 575–583, Mar./Apr. 2010.

[12] A. V. Jouanne, D. A. Rendusara, P. N. Enjeti, and J. W. Gray, "Filtering techniques to minimize the effect of long motor leads on PWM inverter-fed AC motor drive systems," *IEEE Trans. Ind. Appl.*, vol. 32, no. 4, pp. 919–926, Jul. 1996.

[13] H. Bhowmik and K. W. Tou, "Experimental study of transient natural convection heat transfer from simulated electronic chips," *Exp. Thermal Fluid Sci.*, vol. 29, no. 4, pp. 485–492, 2005.

[14] M. Musallam, C. M. Johnson, C. Yin, H. Lu, and C. Bailey, "Real-time life expectancy estimation in power modules," in *Proc. 2nd Electron. Syst.-Integr. Technol. Conf.*, Sep. 2008, pp. 231–236, doi: 10.1109/ESTC.2008.4684355.

[15] S. Yang, D. Xiang, A. Bryant, P. Mawby, L. Ran, and P. Tavner, "Condition monitoring for device reliability in power electronic converters: A review," *IEEE Trans. Power Electron.*, vol. 25, no. 11, pp. 2734–2752, Nov. 2010.

[16] O. S. Senturk, S. Munk-Nielsen, R. Teodorescu, L. Helle, and P. Rodriguez, "Electro-thermal modeling for junction temperature cycling-based lifetime prediction of a press-pack IGBT 3L-NPC-VSC applied to large wind turbines," in *Proc. IEEE Energy Convers. Congr. Expo.*, Sep. 2011, pp. 568–575, doi: 10.1109/ECCE.2011.6063820.

[17] R. J. McGlen, R. Jachuck, and S. Lin, "Integrated thermal management techniques for high power electronic devices," *Appl. Thermal Eng.*, vol. 24, nos. 8–9, pp. 1143–1156, 2004.

[18] T. Frey, A. Stuck, and R. Zehringer, "Liquid cooling device for a high-power semiconductor module," U.S. Patent 5 978 220 A, Nov. 2, 1999.

[19] T. Zywiak and L. J. Bruno, "Cabin air conditioning system with liquid cooling for power electronics," U.S. Patent 7 334 422 B2, Feb. 26, 2008.

[20] S. B. Memory, F. E. Ganaway, C. J. Rogers, A. C. DeVuono, A. Phillips, and Z. Zuo, "Modular cooling system and thermal bus for high power electronics cabinets," U.S. Patent 6 828 675 B2, Dec. 7, 2004.

[21] M. T. Zhang, M. M. Jovanovic, and F. C. Lee, "Design and analysis of thermal management for high-power-density converters in sealed enclosures," in *Proc. Appl. Power Electron. Conf. (APEC)*, Feb. 1997, pp. 405–412, doi: 10.1109/APEC.1997.581482.

[22] P. M. Teertstra, M. M. Yovanovich, and J. R. Culham, "Modeling of natural convection in electronic enclosures," *J. Electron. Packag.*, vol. 128, no. 2, pp. 157–165, 2005, doi: 10.1115/1.2188953.

[23] J. M. Gutierrez-Alcaraz, S. W. H. De Haan, and J. A. Ferreira, "Seawater based cold plate for power electronics," in *Proc. IEEE Energy Convers. Congr. Expo. (ECCE)*, Sep. 2010, pp. 2985–2992, doi: 10.1109/ECCE.2010.5618357.

[24] C.-L. Su, W.-L. Chung, and K.-T. Yu, "An energy-savings evaluation method for variable-frequency-drive applications on ship central cooling systems," *IEEE Trans. Ind. Appl.*, vol. 50, no. 2, pp. 1286–1294, Mar. 2014.

[25] A. B. Sanfiorenzo, "Cooling system design tool for rapid development and analysis of chilled water systems aboard US navy surface ships," M. S. thesis, Dept. Mech. Eng., MIT, Cambridge, MA, USA, 2013.

[26] H. V. Xuan, D. Lahaye, S. O. Ani, H. Polinder, and J. A. Ferreira, "Electrical generators for maritime application," in *Proc. Int. Conf. Elect. Mach. Syst. (ICEMS)*, Aug. 2011, pp. 1–6.

[27] S. S. Kang, "Advanced cooling for power electronics," in *Proc. 7th Int. Conf. Integr. Power Electron. Syst. (CIPS)*, Mar. 2012, pp. 1–8.

[28] J. Schulz-Harder, "Review on highly integrated solutions for power electronic devices," in *Proc. 5th Int. Conf. Integr. Power Electron. Syst. (CIPS)*, Mar. 2008, pp. 1–7.

[29] S. Taieb, L. A. Hatem, and J. Balti, "Natural convection in an asymmetrically heated vertical channel with an adiabatic auxiliary plate," *Int. J. Thermal Sci.*, vol. 74, pp. 24–36, Dec. 2013.

[30] K. Ma, "Electro-thermal model of power semiconductors dedicated for both case and junction temperature estimation," in *Power Electronics for the Next Generation Wind Turbine System*, 2nd ed. Cham, Switzerland: Springer, 2015, pp. 139–143.

[31] K. Ma, Y. Yang, and F. Blaabjerg, "Transient modelling of loss and thermal dynamics in power semiconductor devices," in *Proc. Energy Convers. Congr. Expo. (ECCE)*, Sep. 2014, pp. 5495–5501.

[32] Y. S. Muzychka, J. R. Culham, and M. M. Yovanovich, "Thermal spreading resistance of eccentric heat sources on rectangular flux channels," *J. Electron. Packag.*, vol. 125, no. 2, pp. 178–185, 2003.

[33] Y. A. Cengel, "Natural convection," in *Heat Transfer: A Practical Approach*, 2nd ed. New York, NY, USA: McGraw-Hill, 2004, pp. 459–500.

[34] A. Bejan, *Convection Heat Transfer*. Hoboken, NJ, USA: Wiley, 2013, doi: 10.1002/9781118671627.

[35] S. W. Churchill and H. H. S. Chu, "Correlating equations for laminar and turbulent free convection from a vertical plate," *Int. J. Heat Mass Transf.*, vol. 18, no. 11, pp. 1323–1329, 1975.

[36] A. Demuren and H. Grotjans, "Buoyancy-driven flows—Beyond the boussinesq approximation," *Numer. Heat Transf., B, Fundamentals*, vol. 56, no. 1, pp. 1–22, 2009.

[37] D. D. Gray and A. Giorgini, "The validity of the boussinesq approximation for liquids and gases," *Int. J. Heat Mass Transf.*, vol. 19, no. 5, pp. 545–551, 1976.

[38] W. M. To and J. A. C. Humphrey, "Numerical simulation of buoyant, turbulent flow—I. Free convection along a heated, vertical, flat plate," *Int. J. Heat Mass Transf.*, vol. 29, no. 4, pp. 573–592, 1986.

[39] Y. A. Cengel and T. H. Ngai, "Cooling of vertical shrouded-fin arrays of rectangular profile by natural convection: An experimental study," *Heat Transf. Eng.*, vol. 12, no. 4, pp. 27–39, 1991.

FAISAL WANI received the master's degree in electrical engineering from the Delft University of Technology, The Netherlands, in 2016, and the master's degree in wind technology from the Norwegian University of Science and Technology, Norway.

He is currently pursuing the Ph.D. degree with the Delft University of Technology. Prior to this, he was an Engineer at Power Grid Corporation of India Ltd. His research areas include ocean energy and wind energy conversion systems, with emphasis on electrical machine modeling and reliability of electrical drives.

UDAI SHIPURKAR received the M.Sc. degree in electrical engineering from the Delft University of Technology, The Netherlands, in 2014, where he is currently pursuing the Ph.D. degree. His research focuses are the design for reliable power production in wind turbine generator systems.

JIANNING DONG received the B.S. and Ph.D. degrees in electrical engineering from Southeast University, Nanjing, China, in 2010 and 2015, respectively. He was a Post-Doctoral Researcher at the McMaster Automotive Resource Centre, McMaster University, Hamilton, ON, Canada. Since 2016, he has been an Assistant Professor at the Delft University of Technology, The Netherlands. His research interests include the design, modeling, and control of electromechanical systems.

HENK POLINDER received the Ph.D. degree from the Delft University of Technology, The Netherlands. Since 1996, he has been an Assistant/Associate Professor at the Delft University of Technology in the field of electrical machines and drives. He worked part-time in industries, at wind turbine manufacturer Lagerwey from 1998 to 1999, at Philips CFT in 2001, and at ABB Corporate Research, Västerås, in 2008. He was a Visiting Scholar at Newcastle University, Newcastle upon Tyne, in 2002, at Laval University, Quebec, in 2004, at The University of Edinburgh in 2006, and at the University of Itajubá in 2014. He has authored and co-authored of over 250 publications. His main research interests are electric drive systems for maritime and ocean energy applications.